EVS27
Barcelona, Spain, November 17-20, 2013

DC internal resistance during charge: analysis and study on $LiFePO_4$ batteries

D. Anseán[1], V.M. García[2], M. González[1], J.C. Viera[1], C. Blanco[1], J.L. Antuña[1]
[1]*University of Oviedo, Department of Electrical Engineering, Campus de Gijón, s/n, Módulo 3, 33204, Gijón, Asturias, Spain, anseandavid.uo@uniovi.es*
[2] *University of Oviedo, Department of Physical and Analytical Chemistry, Campus de Gijón, s/n, Edificio Polivalente, 33204, Gijón, Asturias, Spain*

Abstract

DC internal resistance (IR) is considered one of the most important parameters of a battery, as it is used to evaluate the battery's power performance, energy efficiency, aging mechanisms or equivalent circuit modeling. In electric vehicle (EV) applications, the IR during charge gives also essential information related with regenerative braking and dynamic charge efficiency. In this work, we tested four lithium iron phosphate batteries (LFP) ranging from 16 Ah to 100 Ah, suitable for its use in EVs. We carried out the analysis using three different IR methods, and performed the tests at three charging rates (nominal, mid and high) through several states of charge (SOC). In this paper, we study the IR dependency with battery's capacity, SOC and the charging rate; also, the convenience of using a certain IR method is analyzed. Furthermore, the main results are put into context for practical EV applications, to enhance the design of battery management systems (BMS) in relation with the system's energy efficiency.

Keywords: Charging DC internal resistance, measurement methods, lithium iron phosphate

1 Introduction

Some of the most important features and specifications of electric vehicles (EV) are determined by the battery. Automotive manufacturers seek for batteries with optimum characteristics: energy density, thermal management, safety and cost. Additionally, the batteries condition the EVs range and acceleration. While the range can be increased by adding more capacity, acceleration can be either increased by adding more capacity or selecting batteries with higher power density (W/kg). Therefore, power density plays a significant role when choosing the battery for an EV.

In order to characterize the power density of a battery, the internal resistance (IR) has to be evaluated. Battery IR is a key parameter, and considered one of the most important characteristics of a battery: it is directly linked to the power performance and specific power (W/kg), energy efficiency, ability to perform fast charging and regenerative braking, and is also related to physical degradation [1,2]. All these set of parameters are therefore crucial for the correct functioning of an EV and its battery management system (BMS).

The IR of a battery is a complex system, showing capacitive, resistive and inductive behavior interrelated among them [3]. In addition, it is also dependent on several factors: from its capacity, constructive materials and its geometry, to physical and electrochemical phenomena [4-6]. As a consequence, the IR of a battery changes with the charge/discharge current rates, state of charge (SOC), state of health (SOH), temperature, and

previous history. Battery aging mechanisms are also related with the IR: in essence, the IR increases with aging [2].
In order to analyze the resistance of a battery, various methods have been proposed; DC pulse current [6-7], voltage curve difference [8-10], or the method proposed by the USABC [11], which has been widely adopted by battery manufacturers [7]. These methods share the advantages of easiness to implement, simple calculations, and give realistic results. A summary of the advantages and characteristics can be found in [12]. Another commonly used method is the electrochemical impedance spectroscopy (EIS). This is an advanced method to analyze the dynamic behavior of batteries [13], although it requires a specialized set of instruments, it takes long testing time [6], and could give unrealistic low internal resistance values [14]. It is important to mention that the IR of a battery is also a function of the method of determination used [3,6,12].
In this work, we present the IR results obtained from four fresh lithium ion phosphate (LFP) batteries during charge. The batteries (European and Chinese manufactures) range from 16 Ah to 100 Ah of capacity. The primary aim is to investigate the IR dependency of the four batteries on various conditions: different SOC and different charging current rates, evaluated with three IR methods selected.
We focus our study during charge, and the results are useful to evaluate and discuss the IR dependencies, their implications for fast charging, regenerative braking, battery dimensioning, energy efficiencies, and even battery modeling. This work complements our previous study on IR methods [12], in which we performed similar experiments, during discharge.

2 Theoretical background

The IR of a battery is defined as the opposition to the flow of an electric current within a battery. When the cell is at open circuit, and no current flows, the voltage is given by:

$$E = E_{OCV} \qquad \textit{(Eq. 1)}$$

where E is the voltage of the battery, and E_{OCV} the open circuit voltage (OCV), which represents the thermodynamic limitations on the performance of the battery [8].

When the battery is connected to a power supply, thus charging, the voltage across the cell increases, due to several sources of polarization [6];

$$E = E_{OCV} + \eta_{ohmic} + \eta_{Ch.Tr} + \eta_{diff} \qquad \textit{(Eq. 2)}$$

where η_{ohmic} is the ohmic polarization, resulting both from electronic and ionic resistance of the battery, which includes: electrolyte conductivity, the electrical connections (terminals, current collectors, weld joints and contacts in electrodes) and the separators and contact resistances. The charge transfer or activation polarization $\eta_{Ch.Tr}$ is the energy associated with chemical reactions which occur during the electrode reactions, and η_{diff} is the diffusion polarization, which occurs due to mass transport limitations in the electrolyte and electrode materials [6,8,15].
Fig. 1 shows the evolution of the voltage curve of a battery under a charging current step. The analysis of this curve is essential, because it provides the electrochemical details of the battery polarization sources, described in *Eq. 2*. The time domain of a battery is in a wide range, from microseconds up to hours [13], and the range of time is related to each source of polarization (see Fig. 1).
The dynamic behavior, and therefore the IR of a battery, is influenced by both internal and external parameters. The internal parameters include the battery's SOC, SOH and the design parameters, including its chemistry and quantity of active materials. External parameters are the temperature, current rate and the history of the battery [13,15]. In addition, the temperature strongly influences most of the battery parameters, and the aging processes increase the IR of batteries [2].

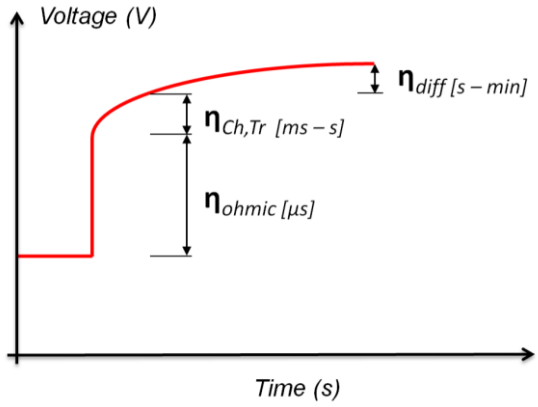

Fig. 1. System response of a battery during charge

	Cell#1	Cell#2	Cell#3	Cell#4
Nominal parameters (C/2)	16Ah	42 Ah	60 Ah	100 Ah
Maximum continuous charge	80 A (5 C)	42 A (1 C)	180 A (3 C)	200 A (2 C)
Cycle life	>2,000 cycles	>3,000 cycles	>1,500 cycles	>2,000 cycles
Cell weight	500 g	1,000 g	2,000 g	3,200 g
Cell geometry	Cylindrical	Pouch	Prismatic	Prismatic
DC internal resistance	<8 mΩ	-	<2.0 mΩ	<0.9 mΩ
Internal resistance method	-	-	-	1 kHz, AC
Country	China	Finland	China	China

Table 1. Summary of the manufacturer's main characteristics of the tested batteries

In summary, the IR of a battery is a complex system, and it is dependent on many parameters, both internal and external. Therefore, an accurate internal resistance study has to take into account all the aforementioned battery characteristics.

3 Experimental

Prior to perform the IR experiments, all the selected batteries are subjected to a conditioning test sequence. These tests are performed according to the USABC conditioning tests [11], in order to determine the effective capacity of the testing batteries.

Once the conditioning stage is completed, the IR experiments start. To obtain the IR of the batteries under various conditions, different charging currents are selected, varying from nominal, mid and high rates. Depending on the battery specifications, nominal charging currents are C/2, medium currents are within the 1C - 2C range, and high are 3C or above. For security reasons, all the tests are performed within the safety limits of the batteries, specified in the characteristics provided by the manufacturer (see Table 1.). All the IR experiments are carried out at various SOC, in order to obtain a specific IR distribution with the state of the cell.

3.1 Selected techniques for battery DC internal resistance determination

Although various IR techniques are found in the literature [3,6-11,15], in this work we selected three commonly used IR methods. These methods slightly differ from each other in terms of accuracy, but give a wide set of useful results as a whole. A summary of the internal resistance methods used is briefly covered in the following subsections, and more details can be found in our previous work [12].

3.1.1 Voltage Curve Difference (VCD)

Various authors [8-10] propose the calculation of the IR at a particular SOC, by the difference of the voltage curves of a battery, under different currents:

$$R_{I1-I2(SOC)} = \left| \frac{U_{I1(SOC)} - U_{I2(SOC)}}{I_1 - I_2} \right| \qquad (Eq.\,3)$$

Fig. 2 shows an actual example of how the parameters in *Eq. 3* are related to the voltage charging curves.

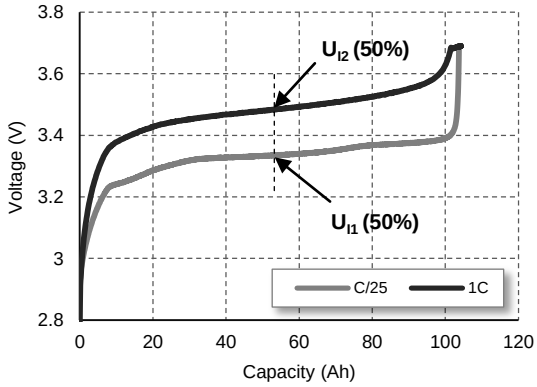

Fig. 2. Charge voltage profiles to calculate the internal resistance with the VCD method

The reference current (I_1) is set to C/25 for all the tests, in order to keep the kinetic effects minimized. The test charging current (I_2) is set to various values, ranging from low currents (C/5) to high currents (up to 5 C).

This method provides an internal resistance value which relates a pseudo equilibrium thermodynamic charge with a kinetic charge, where all the polarizations are activated. The main advantages of this method is its simplicity and rapid execution, but on the other hand is very poor for modeling purposes, the battery temperature is inconstant with charge, and the SOC accuracy is low [12].

3.1.2 USABC

From the USABC manual appendix I [11], the dynamic resistance of a battery is calculated from the ΔV/ΔI measurement between the base current (I_1) and the high test charging current (I_2). The changes in voltage (V_2) are measured at 30 s after the pulse current is applied.

$$IR_{(SOC)} = \frac{\Delta V}{\Delta I} = \left|\frac{V_1 - V_2}{I_1 - I_2}\right| \qquad (Eq. 4)$$

The base current (I_1) was selected to C/4 for all the experiments. This is because C/4 is a charging current capable of activate all the polarization and diffusion effects of the battery, without increasing its internal temperature abruptly. The selected high test charging currents (I_2) ranged from nominal (C/2), medium and high, which can vary with each battery. Each test was evaluated at various fixed SOC.

This IR technique is fairly simple, fast and easy to implement. It also provides good accuracy of the measurements [12].

3.1.3 DC current pulse

The DC current pulse, adopted from Ratnakumar *et al.* [6], performs the IR measurements in true thermodynamic equilibrium. To achieve these conditions, the battery is put in rest at open circuit for 2 h before the 1 min. charging current pulse is injected. To calculate the IR at a defined SOC and pulse magnitude, evaluated at a duration t_s, Equation 5 is used:

$$IR_{(SOC,t_s)} = \frac{U_p - U_{OCV}}{I_p} \qquad (Eq. 5)$$

During the charging pulse, four different voltage measurements are carried out at t_s 100 ms, 2 s, 30 s and 60 s. This enables the calculation of the IR in terms of ohmic, capacitive, reaction polarization and diffusion effects. The current pulse (I_p) varies in range (i.e. C/2, 1C, 3C, etc.) depending on the characteristics of the tested battery.

This IR technique is time-consuming and more complex than the previous, but it has excellent accuracy, data is useful for modeling and it does not affect the battery's temperature since the long resting periods [12].

3.2 Batteries and equipment

The experiments were performed on four fresh batteries. Their chemistry is LFP-based positive electrodes and graphite-based negative electrodes. The battery technology was selected due to its key advantages, i.e. safety, low cost, high cycle-lifetime [1] and the attention that is getting in the EV industry. The studied batteries cover a wide spectrum of features, summarized in Table 1.

For the testing experiments, a modular test bench, developed by the laboratory researchers was used. The equipment has high current capability (± 300 A), fast data acquisition rate (10 µs), temperature and pressure sensors, among other valuable characteristics [16].

The batteries were located in an environmental chamber ($8m^3$) to maintain a constant ambient temperature of 23ºC. The temperatures in both the climate chamber and the battery cases were measured with RTD Pt100 and logged into the modular test bench.

4 Results

Due to the large amount of results obtained from the experiments carried out in this work, we opted to only show the most representative and interrelated results. We consider that this data selection is still large enough to fully analyze and obtain solid conclusions.

Table 2 shows some of the results obtained from the conditioning tests, at nominal rate (C/2) and at C/25. The results of the C/25 measurements provide a practical capacity reference with minimal kinetic effects, close to me maximum capacity attainable [4]. This cause clearly affects Cell#2 and Cell#3, with 11% and 12.7% of capacity increase respectively to the nominal measured value. For the purpose of this work, the results at C/2 are taken as the reference capacity of the battery.

	Cell#1 (16 Ah)	**Cell#2 (42 Ah)**	**Cell#3 (60 Ah)**	**Cell#4 (100 Ah)**
C/25	15.7Ah	46.7Ah	68.9Ah	103.7Ah
Nominal (C/2)	15.5Ah	42.0Ah	61.1Ah	103.1Ah

Table. 2. Charge capacity values during the conditioning tests

4.1 Cell#1 (16 Ah)

In order to perform the voltage curve difference (VCD) IR method, various constant current charging tests have to be performed, as explained in Section 3.1.1. Fig. 3 shows an example of the voltage profiles. It is clear how higher current rates result in higher battery potentials, thus increasing the energy consumption. We can also see that the constant voltage stage is reached at lower capacities when current rates are increased; i.e. at 2C it is reached at 9 Ah, or 55% of SOC. Even if the Cell#1 manufacturer's specification states that fast charges up to 5C (80 A) can be completed, our results show that when charging at that fast rate, the battery immediately locks up to the constant voltage stage (CV), and the current decreases exponentially. Thus charging at those high rates cannot be implemented.

Fig. 4 shows the temperature evolution during charge, at various C-rates. Charging at rates below 1C does not affect the battery temperature, with increases lower than 1ºC. However, when charging above 2C rates, the temperature increases, reaching temperatures over 32ºC.

The charging stages (CC and CV) also affect the battery's temperature behavior: as seen in Fig. 3, the CV stage at 2C is reached at 55% SOC. At that point, as the charging current decreases exponentially, the temperature evolution slows down. It reaches its maximum (32.7ºC) approximately at 75% SOC, and then decreases very rapidly, until it falls to 24ºC when the charging process is finished. Therefore, it is important to evaluate the temperature evolution, because its effects influence the battery IR. Low temperatures tend to increase the IR of a battery, whereas high temperatures tend to decrease it [6,15].

The IR values, evaluated with the three proposed methods, are shown from Fig. 5 - 7.

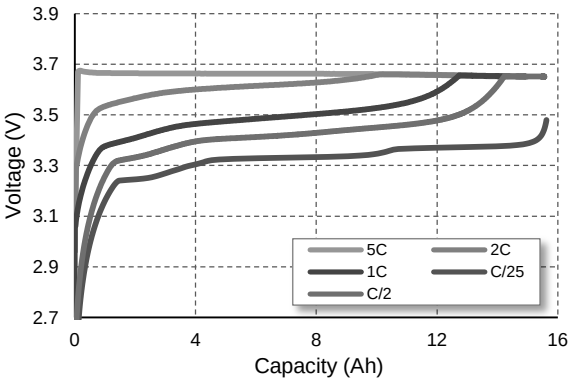

Fig. 3. Charge voltage profiles at various rates (Cell#1)

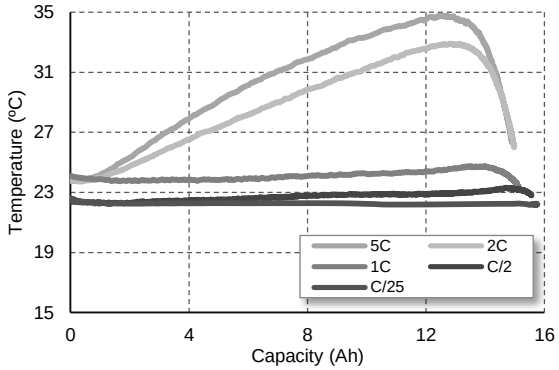

Fig. 4. Temperature evolution during the charge at various rates (Cell#1)

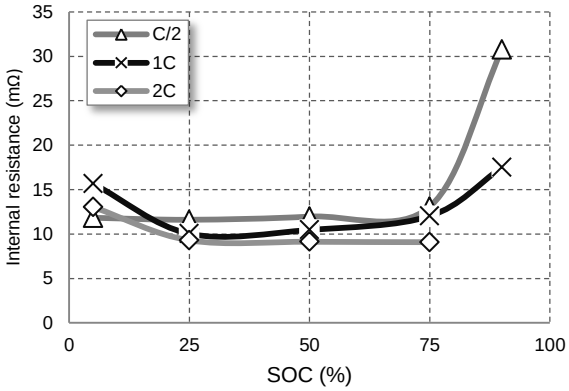

Fig. 5. Internal resistance evolution using the VCD method (Cell#1)

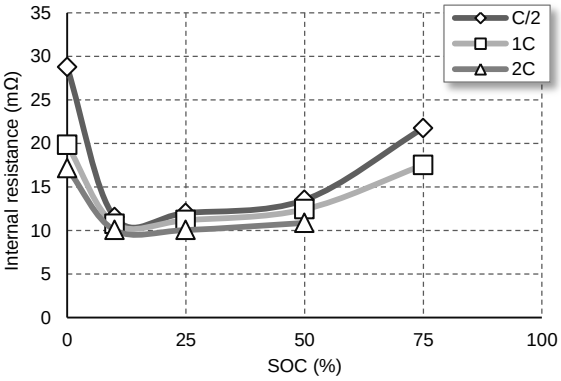

Fig. 6. Internal resistance evolution using the USABC method (Cell#1)

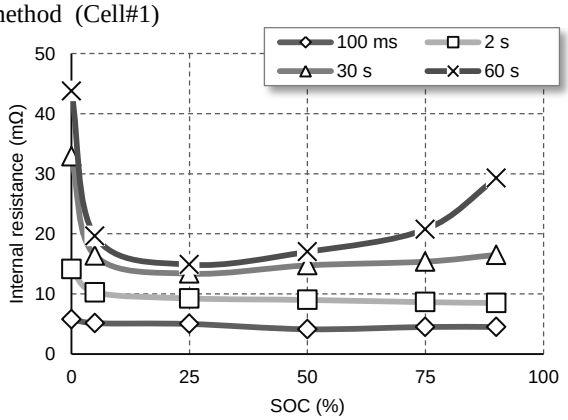

Fig. 7. Internal resistance evolution using the DC current pulse, at C/2 (Cell#1)

In general, the IR evolution with the SOC follows a "U" shape; the highest IR values are both shown at the lowest and highest SOC states. Discrepancies are also more significant at the SOC extremes: that is where both VCD and USABC methods are the least precise. However, in the midrange (25% to 75% SOC), the values remain somewhat similar.

Fig. 6 does not show the IR values at 90% SOC because the battery is already in its CV stage, thus IR cannot be properly analyzed. That is a common limit when charging at fast current rates and high SOC.

Fig. 7 shows the values using the DC pulse method, evaluated at C/2. This method, although the most time consuming and complex, gives the best set of results, in terms of battery dynamics. From Fig. 7 it is also seen that fast data acquisition values (100 ms and 2 s) gives the ohmic and charges transfer values, which are practically constant throughout the battery's SOC. A representative IR value could be indicated at nominal current (C/2) and 50% SOC: ≈10 mΩ.

4.2 Cell#2 (42 Ah)

Cell#2 has some particular characteristics: European made and pouch type. This geometry results in the highest specific energy of 155 Wh/kg in this work, while the other tested batteries remain within the 100 Wh/kg range. Whereas, its maximum operating conditions are more restrict; it is not recommended to perform continuous charge above 1C, and the acquisition price is about two times higher.

The charge voltage profiles at various rates are shown in Fig. 8. From this figure, it is significant the C/25 curve: due to the slow kinetic effects, three plateaus are clearly identified. These effects are directly linked with the graphite negative electrode phase coexistences [4]. Another result is that the attainable capacity at C/25 is 11% higher than at nominal rate (C/2). These two effects reduce the internal resistance VCD method accuracy; the values are calculated from the voltage different SOC points at the reference voltage, C/25. Also notice that the battery CV stage only charges the final 2-3% of the remaining capacity.

The IR values from the VCD method are shown in Fig. 9, where the point at C/2, 50% SOC is higher than its adjacent values.

Fig. 10 shows how the IR values at 50% SOC are reduced as the current increases: from 2.48 mΩ at 2C to 3.72 mΩ at C/2 (35% increase). This effect is found in all the results of this work, and is a common feature in lithium batteries: the IR is a strong function of the current under slow kinetics. On the other hand, under fast dynamics the IR is independent from the charging current.

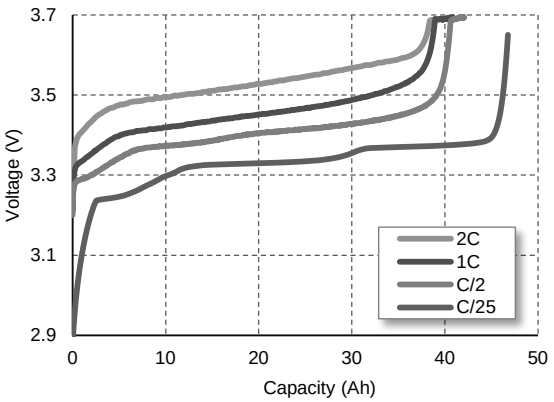

Fig. 8. Charge voltage profiles at various rates (Cell#2)

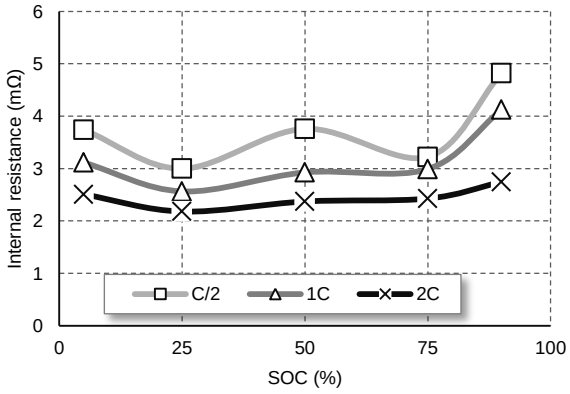

Fig. 9. Internal resistance evolution using the VCD method (Cell#2)

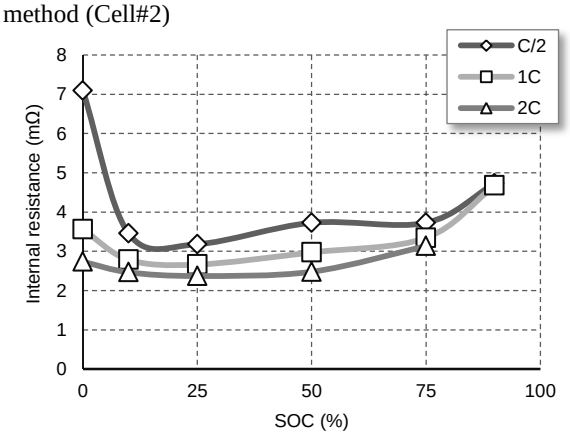

Fig. 10. Internal resistance evolution using the USABC method (Cell#2)

Finally, Fig. 11 shows the results using the DC current pulse, at 1C. The faster dynamic effects are rather constant through the battery's SOC, and remain within the 2 to 2.5 mΩ range. On the other hand, the low dynamic effects, such as the diffusional polarizations have higher values (4 to 6 mΩ) and increase at both extremes of the battery's SOC. Finally, a representative IR value could be indicated at nominal current (C/2) and 50% SOC: ≈3.7 mΩ.

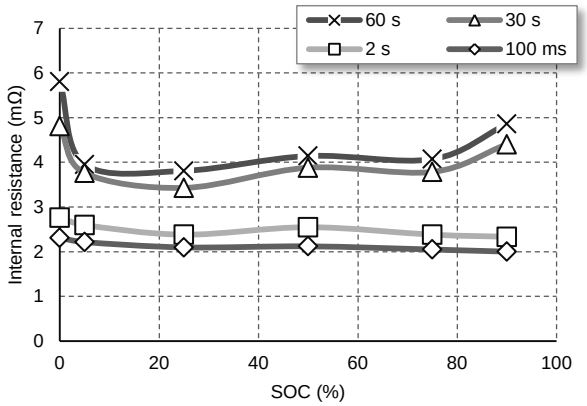

Fig. 11. Internal resistance evolution using the DC current pulse, at 1C (Cell#2)

4.3 Cell#3 (60 Ah)

This battery shows the best fast charging capabilities of the four tested models selected for this work. Charging at 3C (180 A) is attainable, and the temperatures do not rise above 32ºC, even at 3C. It also shows the highest capacity difference (12.7%) between nominal (C/2) and thermodynamic (C/25) charge. The CV stage in this battery charges the last 8% of the capacity at 3C, although is reduced at lower charging currents (5% of total capacity at C/2).

The most significant IR values of Cell#3 are shown from Fig. 12 to Fig. 14. The IR distribution, as seen with the previous batteries, also shows the highest values both at the end and especially at the beginning of the battery SOC. However, the distribution tends to be more constant as the charging rates increase.

The charging current influences the IR values: charging at C/2 gives an IR value of ≈2.7 mΩ, whereas its value at 3C is reduced to ≈2 mΩ, both evaluated at 50% SOC.

Fig. 14 shows the IR values when charging at 3C. Again, the fast dynamic results (100 ms and 2 s) tend to be more constant, although lower SOC shows slightly higher IR values.

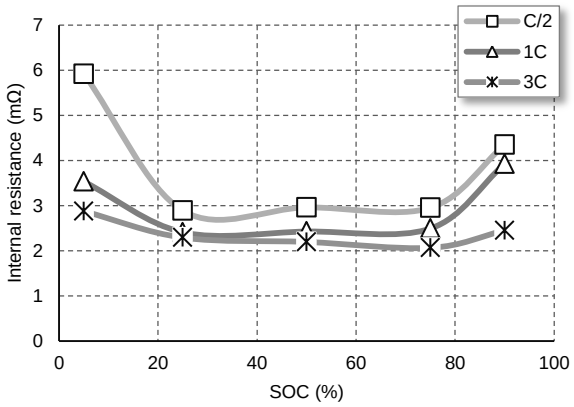

Fig. 12. Internal resistance evolution using the VCD method (Cell#3)

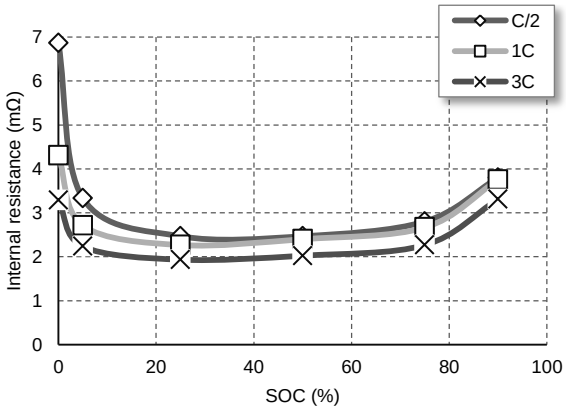

Fig. 13. Internal resistance evolution using the USABC method (Cell#3)

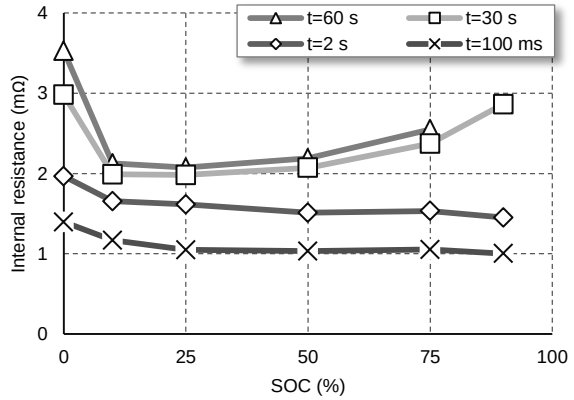

Fig. 14. Internal resistance evolution using the DC current pulse, at 3C (Cell#3)

The IR values obtained at 100 ms remain unchanged under the different charging current rates (nominal-mid-high).

Finally, at nominal charging current (30 A) and 50% SOC, the IR values are within the 2.7 mΩ values.

4.4 Cell#4 (100 Ah)

Cell#4 can be charged at a maximum 2C (200 A) rate. At this high current, the battery's temperature reaches a maximum of 35ºC at 98% SOC, and the CV stage charges the last 6% remaining capacity. At nominal rates (C/2), the figures are less demanding: the temperature has a maximum of 25ºC, and the charge process is practically performed at CC, with only the last 1-2% of capacity filled at CV.

From Fig. 15 to Fig. 17 the most significant IR values are shown. The results are similar as the previously exposed: for slow dynamics, the highest IR values are found at the SOC extremes and higher currents result in smaller IR values. For fast dynamics, the IR values remain constant with SOC and independent of the charging current.

However, there is one difference, which is seen in Fig. 15: the IR values at 5% SOC are the lowest. This may be related with the IR method used. As previously stated, this method is less accurate at the lowest and highest SOC of the battery. The values calculated from 25% to 75% are comparable as those obtained under the USABC and DC pulse current methods.

The IR values at nominal rate (C/2), 50% SOC are within the 1.8 mΩ range.

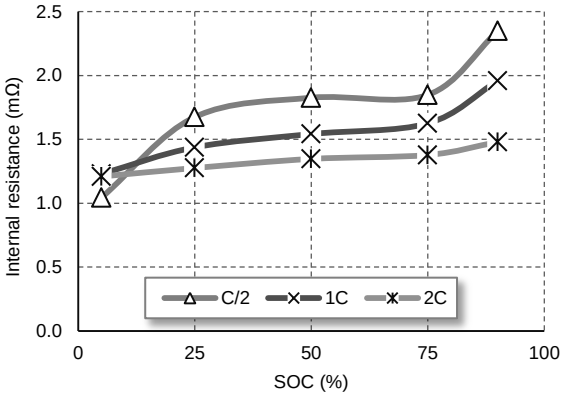

Fig. 15. Internal resistance evolution using the VCD method (Cell#4)

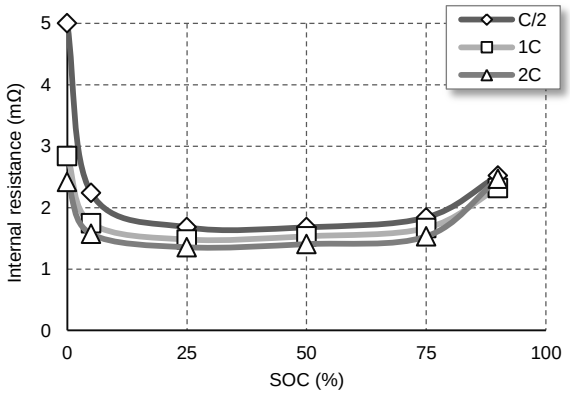

Fig. 16. Internal resistance evolution using the USABC method (Cell#4)

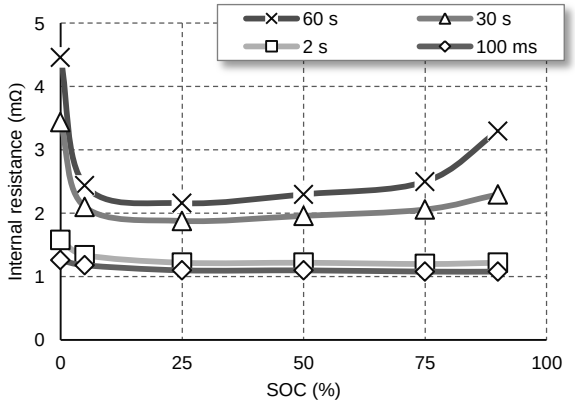

Fig. 17. Internal resistance evolution using the DC current pulse, at C/2 (Cell#4)

5 Discussion

This work presents the charging IR results obtained from four fresh LFP batteries from 16 Ah to 100 Ah, suitable for its use in EVs. The IR has been calculated at various SOC and current rates (nominal, mid and high), using three internal resistance methods. We found that the IR of a battery depends on various factors: SOC, charging current, battery dynamics, and in less degree, to the IR method. These results are in concordance with previous studies, as shown in [3-7,10,12-15].

As seen in the results, at slow dynamics the IR as a function of SOC has a flattened parabolic shape, with the highest values at full discharge and in less degree, when the full charge is reached. However, the IR during most of the SOC (approximately from 15 to 75 % SOC) remains relatively constant, and at lower values, around 1/3 of its maximum. This effect may be understood in terms of kinetics and mass transport effects, as the reversible process become more facile, when concentration of products are identical, i.e., at 50% SOC [6].

The charging current rate and its time length also play a significant role in the IR evolution. This effect is dependent of the battery dynamics: under the ohmic effects, which are usually ranged within µs, the IR is not affected neither by the current or the SOC; so, it remains invariant. However, slower dynamics, containing both charge transfer and diffusion effects, are SOC and current dependent [6]. The general effects under slower dynamics tend to decrease the IR of a battery with higher currents.

The IR also changes with the SOC, increasing at the extremes, especially under the diffusion effects. This is shown in the results section.
Regarding the IR method, each one has advantages and disadvantages. Some methods are easier to implement or less time consuming, while others, such as the DC pulse, can separate the ohmic, charge transfer and mass transfer component polarizations. Therefore, the IR method must be selected according to the testing time and equipment, and to the data which are desired to be obtained. A detailed summary of the internal resistance methods and its main characteristics is out of the scope of this work, but it can be found in [12].
The IR of a battery is related with its capacity. In general, for the same type of technology and battery application (i.e. high energy or high power) higher capacities result in lower IR values. This is demonstrated in our results. However, since the IR of a battery depends on its electrochemistry, constructive materials, geometry or application to name a few [1], the IR values can vary in a broad range. Burke *et al* [17] show this fact with a summary of thirteen IR values of different batteries.
For practical applications in EVs, the results obtained in this work can be applied to enhance the design of battery management systems (BMS) and energy management systems (EMS). The BMS should be capable of precisely calculate the IR of a battery, and in this work different methods are studied. Moreover, since the IR of a battery is SOC and current dependent, BMS and EMS should be capable of detect this dependency, and proceed to take action: the EMS controls the energy flow dynamically to minimize losses; so, it must consider the battery dynamics. The range between 15 to 75% SOC is where the IR is lower; thus, charging or regenerative braking is more efficient within this SOC range. Also, when the battery is operated at either low or high SOC, the power capability is limited and the energy efficiency lower. Therefore, algorithms should decrease the power capability requirements at higher and lower SOC. Battery dynamics should also be detected by the BMS, since fast dynamic effects have different behavior, and are not SOC and current dependent.
Although the dependence with temperatures has not been studied in detail in this work for simplicity, temperature also plays a significant role in the IR. Therefore battery temperatures should be evaluated and controlled by the BMS. It is crucial to avoid unnecessary dendrite formation and safety risks: the BMS should control the charging current rates, and the temperature, especially when it is low.
Dendrite formation is a well-known and hazardous phenomenon which affects negatively the battery functioning. It can cause the separator to disconnect and become isolated from the electrolyte, and in some instances pierce through the separator [18]. These effects can result in a short circuit and thermal runaway in the battery. The factors that cause these unwanted phenomena can be divided into constructive and operative: constructive are the nature of the electrolyte and the ratio between anode and cathode capacities, whereas the operative factors are the temperature, the charging rate and battery aging [2,4,18]. Lower temperatures and high charging rates, especially at high SOC are very dangerous. In addition, the risks tend to increase as the battery ages. Therefore, it is crucial to follow the manufacturer's technical specifications at low temperatures and fast charging.
The IR is also dependent on its ageing mechanisms. As stated by many authors [2,4-6,15,18] the battery's IR tend to increase as it ages, and its SOC dependency also changes significantly [15]. In this regard, we will continue this present work, and carry out further tests to analyze these ageing effects.

6 Conclusion

In this work, the internal resistance of four LFP batteries from 16 Ah to 100 Ah was studied during charge. It was evaluated the IR dependency of the batteries on variable testing conditions: SOC, charging current rate and IR measurement method.
The results indicate that the IR of a battery under slow dynamics, changes with its SOC, showing the lowest values around its low to mid charge, and the highest IR values at both SOC extremes. It is also shown that the IR is reduced when the charging current is increased. On the other hand, fast dynamics are SOC and current independent.
The measurement methods also exhibit different capabilities, and its properties have to be taken into account when the IR of a battery must be evaluated. Moreover, results show that batteries with higher capacities have smaller IR values.
System designers can utilize the results obtained in this work to enhance the efficiency of a final battery system, i.e. an EV. For instance, fast charging, long regenerative braking or power capability is more efficient when the battery is in the mid SOC.

Therefore, it is crucial in a BMS to properly analyze and quantify the IR of a battery frequently.
Further studies will be focused on how the IR evolves as the battery ages.

Acknowledgments

The authors would like to thank the Spanish Ministry of Science and Innovation (MICINN) who provided the funding (TEC2009-12552) for this work.

References

[1] W.J. Zhang, *Structure and performance of $LiFePO_4$ cathode materials: A review*, Journal of Power Sources, ISSN 0378-7753, 196 (2011), 2962-2970

[2] J. Vetter et. Al., *Ageing mechanisms in Lithium-ion batteries*, Journal of Power Sources, ISSN 0378-7753, 147(2005), 269-281

[3] H.G. Schweiger et. Al., *Comparison of several methods for determining the internal resistance of lithium ion cells*, Sensors, ISSN 1424-8220, 10 (2010), 5604-5625

[4] M. Dubarry, C. Truchot, B.Y. Liaw, *Synthesize battery degradation modes via a diagnostic and prognostic model*, Journal of Power Sources, ISSN 0378-7753, 219 (2012), 204-216

[5] A.J. Bard, L.R. Faulkner, *Electrochemical methods, fundamentals and applications*, 2nd edition, ISBN 0-471-04372-9, John Wiley & Sons, 2001

[6] B.V. Ratnakumar et. Al., *The impedance characteristics of Mars Exploration Rover Li-ion batteries*, Journal of Power Sources, ISSN 0378-7753, 159 (2006), 1428-1439

[7] S. Zhao, A.F. Burke et Al., *A measurement method for determination of dc internal resistance of batteries and supercapacitors*, Electrochemistry Communications, ISSN 1388-2481, 12 (2010), 242-245

[8] T.B. Reddy, *Linden's Handbook of Batteries, 4th edition*, ISBN 978-0-07-162421-3, McGraw Hill, 2011

[9] M. Dubarry et. Al, *Evaluation of commercial lithium-ion cells based on composite positive electrode for plug-in hybrid electric vehicle applications. Part I: nitial characterizations*, Journal of Power Sources, ISSN 0378-7753, 196 (2011), 10328-10335

[10] M.A. Roscher, J. Vetter, D.U. Sauer, *Characterization of charge and discharge behavior of lithium ion batteries with olivine based cathode active material*, J. of Power Sources, ISSN 0378-7753, 191 (2009)

[11] United States Advanced Battery Consortium (USABC). *Electric Vehicle Battery Test Procedures Manual*, January 1996. http://www.uscar.org/guest/article_view.php?articles_id=86, accessed on 2013-06-25

[12] D. Anseán et. Al, *Measurement and study of DC internal resistance in $LiFePO_4$ batteries*, European Electric Vehicle Congress, 2012

[13] A. Jossen, *Fundamentals of battery dynamics*, Journal of Power Sources, ISSN 0378-7753, 154 (2006) 530-538

[14] H. Culcu et. Al, *Internal resistance of cells of lithium battery modules with FreedomCAR model*, World Electric Vehicle Journal, ISSN 2032-6653, 3 (2009)

[15] W. Waag, S. Käbitz, D.U. Sauer, *Experimental investigations of the lithium-ion battery impedance characteristic at various conditions and aging states and its influence on the applications*, Applied Energy, ISSN 0306-2619, 102 (2013) 885-897

[16] J.L. Antuña et. Al, *Advanced modular test system for traction batteries*, Advanced Automotive Batteries, AABC Europe, 2011

[17] A. Burke, M. Miller, *The power capability of ultracapacitors and lithium batteries for electric and hybrid vehicle applications*, Journal of Power Sources, ISSN 0378-7753, 196 (2011) 514-522

[18] V. Agubra, J. Fergus, *Lithium ion battery anode aging mechanisms*, Materials, ISSN 1996-1944, 6 (2013), 1310-1325

Authors

David Anseán received the B.Sc. degree in Electronics Engineering from the University of Granada, Spain, in 2007. After gaining some industry experience in Basingstoke, UK, and Berkeley, CA, USA, in 2010 he joined the University of Oviedo, Spain, where he received the M.Sc. degree in Electrical Engineering in 2011, and where he is currently working towards the Ph.D. degree. His research interests include lithium ion batteries, particularly for its use in electric vehicles.

Víctor Manuel García is Professor in the area of Physical Chemistry at the University of Oviedo, Spain, with a doctorate in Quantum Chemistry and expertise in Theory of Electronic Separability. For several years his research interest has been focused on applied aspects of electrochemistry, either in batteries or corrosion. His research is coupled with an intense dedication to chemical education.

Manuela González received the M.Sc. and the Ph.D. degrees in Electrical Engineering from the University of Oviedo, Spain, in 1992 and 1998, respectively. She is the founder and head of the Battery Research Laboratory in the Department of Electrical and Electronic Engineering, at University of Oviedo. Her research interests include battery management systems for new battery technologies and fast chargers for traction applications.

Juan Carlos Viera received the M.Sc. degree in Electrical Engineering from the University of Technology (ISPJAE), Havana, in 1992 and the Ph.D. degree in Electrical Engineering from the University of Oviedo, Spain, in 2003. He is currently an Assistant Professor in the Department of Electrical and Electronic Engineering, at the University of Oviedo, Spain. His research interests include battery management systems, battery testing, fast-charging among others.

Cecilio Blanco received the M.Sc. and Ph.D. degrees in Electrical Engineering from the University of Oviedo, Spain, in 1989 and 1996 respectively. In 1989 he joined the Department of Electrical Engineering at the University of Oviedo, where he is currently an Associate Professor. His research interests include battery fast charging, battery modeling and discharge lamp modeling.

José Luis Antuña received the M.Sc. in Industrial Electronic Engineer from the University of Oviedo, Spain, in 2007. He had a working grant at HC energy company during 2008. He also worked as researcher recycling industrial waste at School of Mines in 2009 and 2010. He is currently working towards the Ph.D. degree and as a researcher at the Battery Research Laboratory at University of Oviedo.